

# Perceptual disturbances predicted in zero-g through three-dimensional modeling

Jan E. Holly

*Department of Mathematics, Colby College, Mayflower Hill Drive, Waterville, ME 04901, USA*

*Tel.: +1 207 872 3202; Fax: +1 207 872 3801; E-mail: jeholly@colby.edu*

Received 7 October 2002

Accepted 28 January 2003

**Abstract.** Perceptual disturbances in zero-g and 1-g differ. For example, the vestibular coriolis (or “cross-coupled”) effect is weaker in zero-g. In 1-g, blindfolded subjects rotating on-axis experience perceptual disturbances upon head tilt, but the effects diminish in zero-g.

Head tilts during centrifugation in zero-g and 1-g are investigated here by means of three-dimensional modeling, using a model that was previously used to explain the zero-g reduction of the on-axis vestibular coriolis effect. The model’s foundation comprises the laws of physics, including linear-angular interactions in three dimensions.

Addressed is the question: In zero-g, will the vestibular coriolis effect be as weak during centrifugation as during on-axis rotation? Centrifugation in 1-g was simulated first, with the subject supine, head toward center. The most noticeable result concerned direction of head yaw. For clockwise centrifuge rotation, greater perceptual effects arose in simulations during yaw counterclockwise (as viewed from the top of the head) than for yaw clockwise. Centrifugation in zero-g was then simulated with the same “supine” orientation. The result: In zero-g the simulated vestibular coriolis effect was greater during centrifugation than during on-axis rotation. In addition, clockwise-counterclockwise differences did not appear in zero-g, in contrast to the differences that appear in 1-g.

**Keywords:** Model, self-motion, perception, zero-g, motion sickness, vestibular

## 1. Introduction

Perceptual disturbances in zero-g differ from those in 1-g, but experimental research is much more easily carried out in 1-g. The vestibular coriolis (or “cross-coupled”) effect is an example of a phenomenon that differs between zero-g and 1-g. The vestibular coriolis effect is a perceptual disturbance, of self-motion misperception and/or motion sickness, that occurs during rotation if the head is then rotated about a second axis not parallel to the main rotation axis. The effect is much weaker in zero-g [10,22]. Useful would be a method to explain and predict perceptual disturbances in zero-g based upon experimental research in 1-g and limited research in zero-g.

Physics always forms the foundation for explaining perceptions of self-motion. Sometimes an additional

explanation is necessary to explain a particular phenomenon, for example using time constants of perception; however, the laws of physics usually explain the basic perception. One well-known example is that of perceived counterclockwise rotation upon deceleration from a clockwise rotation in the dark: because subjects typically report being stationary during the constant-velocity clockwise rotation, the counterclockwise acceleration that is equated with the clockwise deceleration induces a perception of counterclockwise rotation, simply by the laws of physics. Another example is the vestibular coriolis effect in which, for example, a clockwise-rotating subject in the dark who tilts the head rightward will experience a perception of backward pitch motion, or at least of disorientation: according to the laws of physics, even a computer that perfectly interprets accelerations would report backward pitch

in this situation because a rightward-roll head velocity is associated with a backward-pitch acceleration in a clockwise-rotating reference frame, as backward pitch is the cross product of clockwise and rightward-roll angular velocities [12,23].

The key is that the “initial conditions” of perception are not veridical; however, human self-motion perception works well from that point on, interpreting the accelerations according to the laws of physics, at least for short time frames. The “initial conditions” refer to the perceived motion and orientation immediately preceding the movement of interest; in both examples above, the initial conditions of perception are of being stationary and upright. The reason that the initial conditions are not veridical is well-known: over longer time frames, human angular self-motion perception diverges from that of a perfect computer, creating a perception of stationarity in steady-state conditions with no angular acceleration. Because this misperception during steady-state is well-understood, the current topics of interest are the more complex ensuing misperceptions during head movement or whole-body acceleration. In the examples above, the laws of physics explain the basic misperceptions. For short time frames (before time constants associated with human perception become significant factors), the laws of physics have been the most fundamental explanatory and predictive method for understanding self-motion perception [11].

More complex misperceptions of motion have also been explained using the three-dimensional laws of physics as a foundation, and this method holds promise for the zero-g environment as well. In particular, a model implementing the laws of physics and a three-dimensional display of motion has been used to explain why (1) perceived tilt, by an upright subject, changes immediately and quickly during centrifuge deceleration but not during centrifuge acceleration [16,17], (2) forward tumble is perceived during centrifuge deceleration in a centrifuge whose carriage tilts with the roll tilt of the gravito-inertial force vector [17], and (3) the vestibular coriolis effect is much weaker in zero-g than in 1-g [18]. The result about the vestibular coriolis effect depended upon the recognition that the classic explanation, as given above, was incomplete in that it used only angular vectors and not linear vectors such as gravity. Angular-linear interaction has been suggested as a factor in the vestibular coriolis effect [4,39], as have the motor-control consequences of these interactions [21,22]. Angular and linear vectors interact in three-dimensional motion, so all six degrees of freedom – three angular and three linear – were used

in the model, along with all angular-linear interactions according to the laws of physics. The result was that the modeled vestibular coriolis effect showed a more complicated perception than simple pitch. In addition, the modeled vestibular coriolis effect in zero-g was of much smaller magnitude than that in 1-g. Even though the zero-g and 1-g movements were identical, with identical angular accelerations, the linear components of motion and their interaction with the angular components created a perceptual effect much stronger in 1-g. This result still held when time constants for perception were included in the model [19].

Of particular interest are head movements in a centrifuge, because centrifugation is a potential countermeasure against the physiological effects of long-term weightlessness. A recent experimental study, for example, investigated perception during head movements in a centrifuge on the earth with the subject supine and the head at the axis of centrifuge rotation, body aligned radially outward [14]. Perceptual disturbances could be predicted, and were found, because of the same angular velocity cross-coupling that occurs during the classic vestibular coriolis effect.

Investigated here through three-dimensional modeling are vestibular coriolis effects in a centrifuge, in both 1-g and zero-g environments. The subject is considered to be supine with head toward center, and perceptions during each of the two directions of head yaw are investigated. Simulations are carried out in order to explain and predict disorientation in a 1-g environment, and to make predictions about whether vestibular coriolis effects in zero-g will be as weak during centrifugation as during on-axis rotation.

## 2. Methods

Three sets of simulations were carried out: in a centrifuge in 1-g, in a centrifuge in zero-g, and on-axis in 1-g and zero-g.

### 2.1. Motions

For all simulations, the subject was supine with body axis aligned radially with feet away from the center of rotation in such a way that any centripetal acceleration would be in the body’s positive  $z$  direction using the standard head coordinate system (Fig. 1(a), with positive  $x$ ,  $y$ , and  $z$  being directed toward the nose, the left ear, and the top of the head, respectively). For all simulations the centrifuge rotated clockwise at 126.9°/s, a

speed which induces a centripetal acceleration of 0.5 g at a distance of 1 m from the rotation axis. Two head movements were used, each of which was assumed to be preceded by a period of sustained centrifuge rotation with the head in an ear-down position: yaw “clockwise” 90° from left-ear-down to nose-up (Fig. 1(b)), and yaw “counterclockwise” 90° from right-ear-down to nose-up (Fig. 1(c)), each accomplished in 1 s with a sinusoidal angular velocity profile. These motions were chosen because the final position of the head is aligned with the body in both, making comparison easier.

The accelerations experienced by the subject were calculated from the motion profile described above. The angular accelerations throughout the head movement were calculated from the angular velocity of the centrifuge and the head yaw rotation. The gravito-inertial acceleration (GIA) before, during, and after the head movement was calculated as the sum of the centripetal acceleration, which depended upon the radius, and the “gravitational acceleration”, meaning the earth-upward vector indistinguishable by an accelerometer from actual linear acceleration, due to the presence of gravity (for the 1-g runs). Two different radii were used: 0 m to simulate the standard coriolis effect, and 1m to simulate self-motion perception when the “center” of linear acceleration perception is at 1 m from the centrifuge axis, such as when the head is positioned away from the axis or when non-vestibular cues away from the centrifuge axis contribute to the detection of resultant linear acceleration [30,31].

In short, while the steady centrifuge rotation remains clockwise, three sets of simulations were carried out:

- (1) clockwise and counterclockwise yaw in 1-g using radius 1 m,
- (2) clockwise and counterclockwise yaw in zero-g using radius 1 m, and
- (3) clockwise and counterclockwise yaw in 1-g and in zero-g using radius 0 m (to compare with 1 m).

## 2.2. Initial conditions

The initial conditions used the GIA as the interpreted vertical, and the perceived angular and linear velocities were zero. In other words, during constant-velocity rotation of the centrifuge, the subject was simulated as perceiving whole-body tilt orientation in such a way that the direction of the GIA was perceived as vertically upward. (Other possibilities are discussed in the Discussion.) For the zero-g runs at non-zero radius, this means that the subject’s initial perception was of being upright. For the zero-g run at 0 m radius, the subject’s initial perception was also set at “upright”.

## 2.3. Model

The model computed and displayed the three-dimensional motion that would be perceived by a perfect interpreter of the given angular and linear accelerations according to the laws of physics, assuming that the initial perception matched that of the subject, as described above. Head-coincident coordinates were used, in which velocities and accelerations are given in a coordinate system coincident with the head but temporarily fixed relative to the earth so that non-zero velocities can be specified [15]. The transformation from head-coincident coordinates to earth-fixed coordinates was given by the 3-by-3 matrix  $S$  with rows  ${}^h\vec{i}_E$ ,  ${}^h\vec{j}_E$ , and  ${}^h\vec{k}_E$ , representing the earth’s  $\vec{i}$ ,  $\vec{j}$ , and  $\vec{k}$  vectors in head-fixed coordinates. The equations used by the model to implement the laws of physics were

$$\frac{d{}^h\vec{i}_E}{dt} = {}^h\vec{i}_E \times {}^h\vec{\omega}$$

$$\frac{d{}^h\vec{j}_E}{dt} = {}^h\vec{j}_E \times {}^h\vec{\omega}$$

$$\frac{d{}^h\vec{k}_E}{dt} = {}^h\vec{k}_E \times {}^h\vec{\omega}$$

$$\frac{d\vec{r}}{dt} = {}^E\vec{v}$$

$$\frac{d{}^h\vec{\omega}}{dt} = {}^h\vec{\alpha}$$

$$\frac{d{}^E\vec{v}}{dt} = S{}^h\vec{A} - {}^E\vec{g}$$

where pre-superscripts indicate head-coincident ( $h$ ) or earth-fixed ( $E$ ) coordinates, and  $\vec{\omega}$ ,  $\vec{r}$ ,  $\vec{v}$ ,  $\vec{\alpha}$ , and  $\vec{A}$  are angular velocity, linear position, linear velocity, angular acceleration, and GIA, respectively, and  $\vec{g}$  is the “gravitational acceleration”. The continuous inputs to the model were  ${}^h\vec{\alpha}$  and  ${}^h\vec{A}$ . All other variables had their values computed by the model over time, beginning with initial values that were set as described in the section above. For the zero-g runs, the magnitude of “gravity” ( ${}^E\vec{g}$  in the model) was taken to be 0.5 g during centrifuge runs with centripetal acceleration 0.5 g, and 0 g during on-axis runs with no centripetal acceleration.

The computation and the three-dimensional graphics output of the model were developed in Matlab (The MathWorks, Inc. Natick, Massachusetts, USA). The simulations were performed on a Silicon Graphics Workstation and a Windows NT PC. The system of differential equations was solved numerically us-

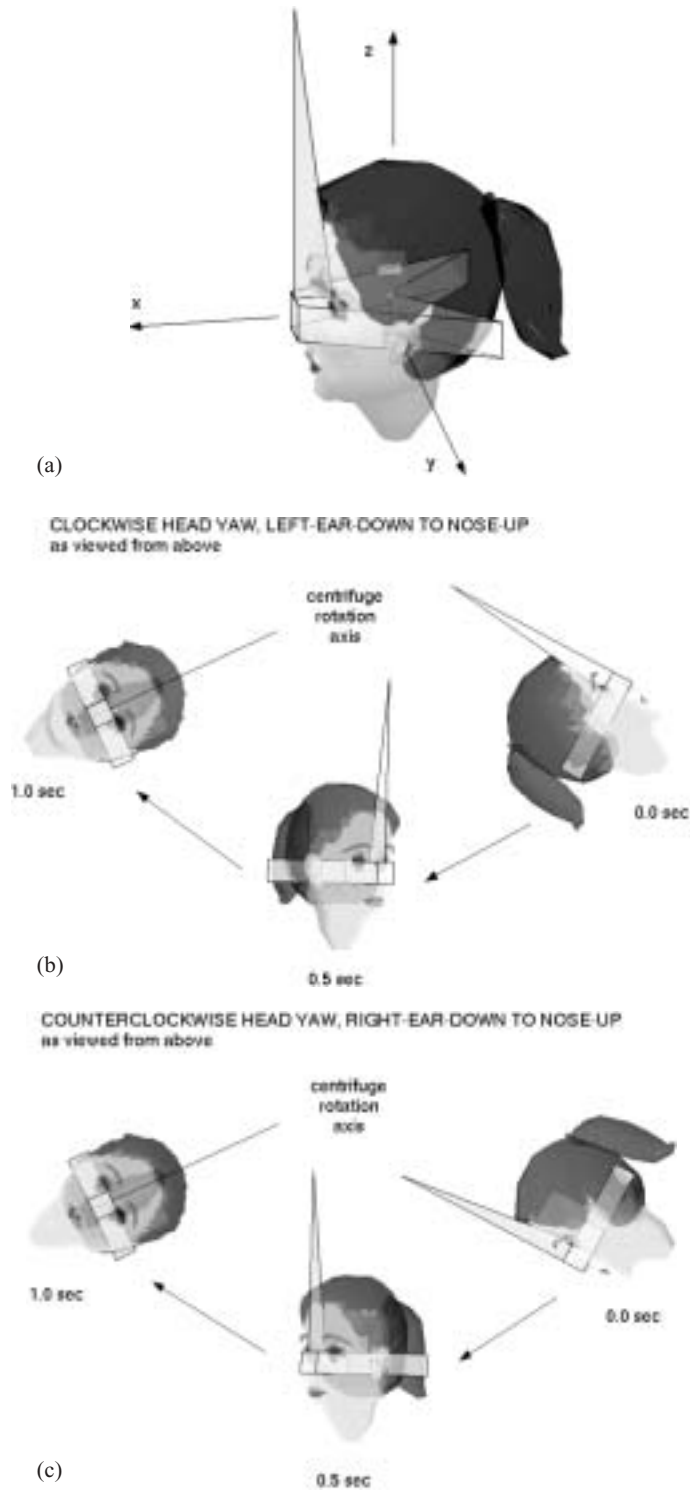


Fig. 1. Three-dimensional graphical conventions and actual head movements. (a) Overlay of head and head coordinate axes onto the polyhedral “head” used for three-dimensional display of motion in later figures. The polyhedral “head” is designed with angular features to enable discrimination of different orientations in time-lapse graphics. (b) Actual head motion during “clockwise” head yaw in a centrifuge, while the centrifuge rotates clockwise as viewed from above. (c) Actual head motion during “counterclockwise” head yaw in the same centrifuge.

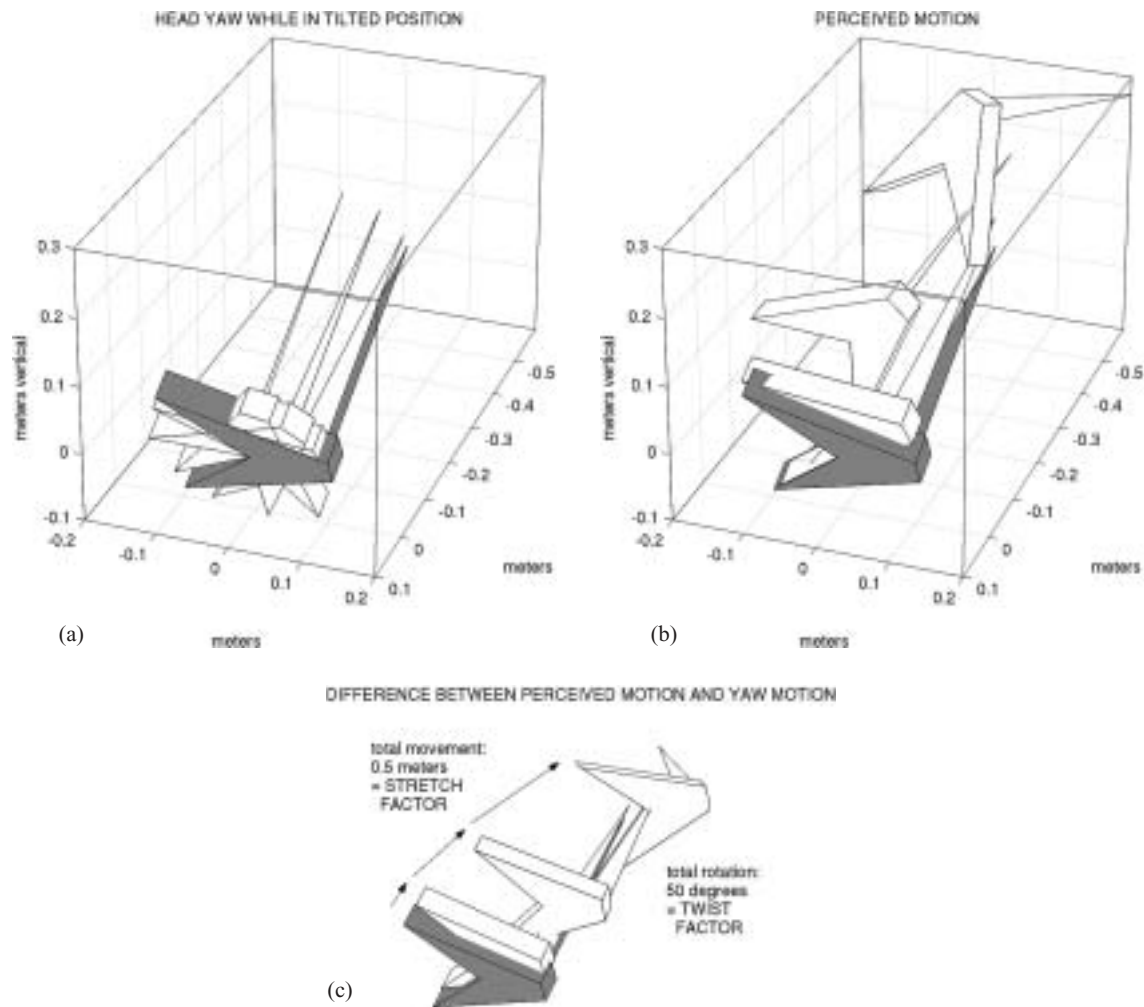


Fig. 2. Graphical illustration of Twist and Stretch Factors. (a) Expected motion that a subject would anticipate perceiving upon turning the head in yaw, if the initial perception is of being partially tilted left-ear-down. The motion is shown in “time-lapse” format with polyhedral “heads” (Fig. 1(a)), the gray head representing the initial perceived position and orientation. Over the example three time steps, the head rotates in rightward yaw while still in a tilted position. (b) Perceived motion that the model might report, same conventions as in a. The head rotates not only in yaw but also pitch backward, and moves head-upward. (c) Three-dimensional difference between the motions in b and a, illustrating the Twist and Stretch Factors, with further technical explanation in the text. The difference does not contain significant yaw because rightward yaw is a similarity between the perceived motion in b and the expected yaw motion in a. However, pitch and roll show up in the difference, and the total Twist Factor was computed from the three-dimensional data to be  $50^\circ$ . Translation also shows up in the difference, and the total Stretch Factor was computed to be 0.5 m.

ing the Runge-Kutta 45 algorithm with absolute tolerance  $10^{-6}$  and relative tolerance  $10^{-3}$ . All simulations were also tested with veridical initial conditions in order to confirm the reliability of the software and error tolerances. The three-dimensional graphics used z-buffering to handle overlapping objects.

#### 2.4. Twist and stretch factors

To compare the magnitude of perceptual disturbance between different simulations, two numerical measures

were used, the Twist Factor and the Stretch Factor.

The Twist Factor (or just “Twist”) is the accumulated angle through which the perceived motion proceeds differently from the expected, simple yaw, motion (Fig. 2). To compute Twist for a perceived motion, first computed is the three-dimensional orientation of the perceived motion relative to the simple yaw motion. Then computed is the magnitude of the angle through which this orientation has rotated in 3-D from one time step to the next; time steps of 0.1 s were used here. The

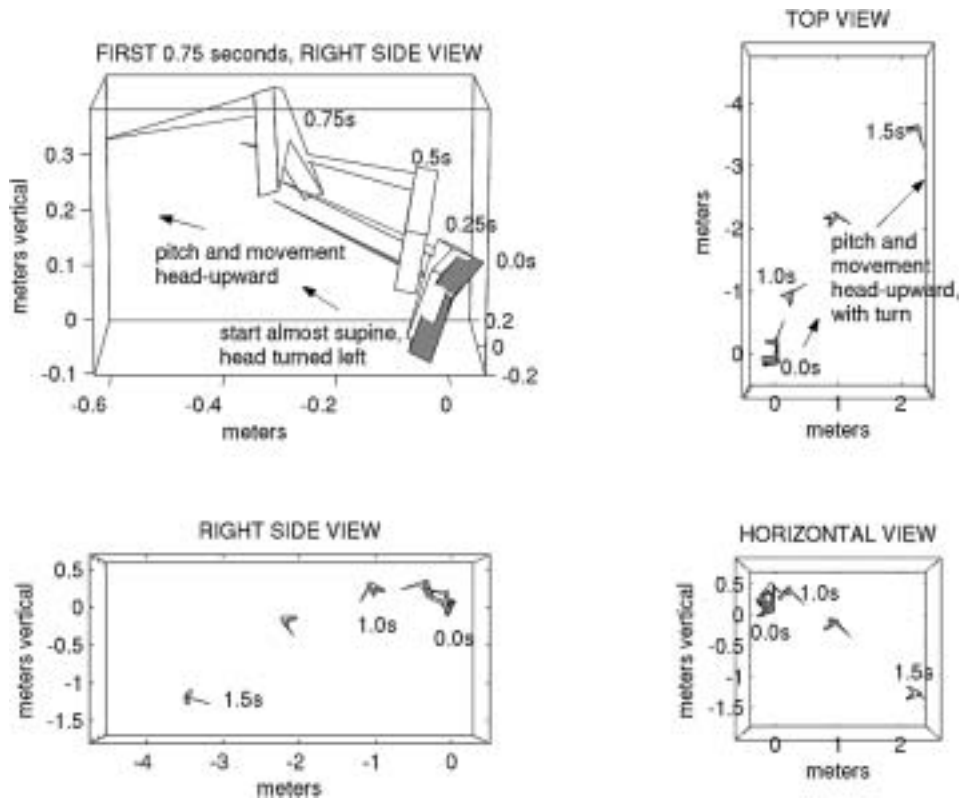


Fig. 3. Clockwise in 1-g: Three-dimensional view of simulated perceived head motion for 1.5 seconds, during 1s of clockwise (left-to-nose-up) head yaw, plus the subsequent 0.5 s, in a centrifuge in a 1-g environment (details in the text). The three-dimensional motion is shown in time lapse format from different angles, with the polyhedral “head” (Fig. 1(a)) shown every 0.25 s, starting in gray at the 3-D origin (0,0,0). In the TOP VIEW, the earth-fixed positive x-axis happens to point downward on the page, and the positive y-axis points to the right. The motion is described further in the text.

Twist at any given time is the sum of these computed “unexpected” rotation angles up to that time.

The Stretch Factor (or “Stretch”) is the accumulated distance that the perceived motion proceeds differently from the expected, simple yaw, motion (Fig. 2). Because yaw motion involves no linear motion, the Stretch for the present perceptions is the length of the path that the perceived motion follows. Stretch was also computed here by integrating using a time step of 0.1 s.

### 3. Results

#### 3.1. In 1-g at radius 1 m

Simulations resulted in three-dimensional displays (Figs 3 and 4) and graphs of Twist and Stretch (1-g curves in Fig. 5) for self-motion perception during 90° head yaw to nose-up while supine in a clockwise-

rotating centrifuge in 1-g, using linear acceleration detection centered at 1 m radius.

The computed three-dimensional perceived motion during clockwise (left-to-nose-up) head yaw (Fig. 3) begins with the initial perception of head turned 90° to the left while mostly supine but tilted somewhat head-up (26.6° to be exact, because the GIA is tilted  $26.6^\circ = \text{Arctan}(0.5 \text{ g}/1 \text{ g})$  since the centripetal acceleration is 0.5 g). The perceived motion then proceeds with clockwise yaw into a backward pitch motion that includes a turn. Notable is the fact that the angular pitch rotation is accompanied by a backward linear motion that could be interpreted as enhancing the pitch perception.

The corresponding motion during counterclockwise (right-to-nose-up) head yaw (Fig. 4) begins with the initial perception of head turned 90° to the right while mostly supine but tilted head-up 26.6°. The perceived motion then proceeds with counterclockwise yaw into a forward pitch motion with a rotation. As in the clockwise-yaw simulation (Fig. 3), the angular pitch rotation is accompanied by an enhancing linear mo-

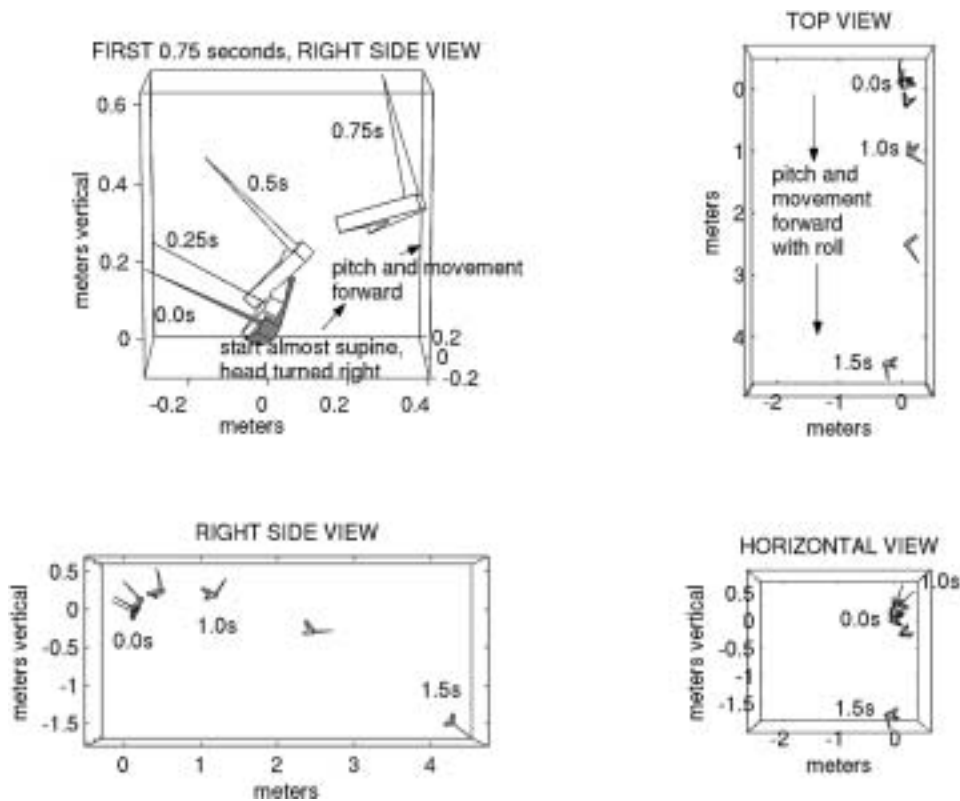


Fig. 4. Counterclockwise in 1-g: Three-dimensional view of simulated perceived head motion for 1.5 seconds, during 1 s of counterclockwise (right-to-nose-up) head yaw, plus the subsequent 0.5 s, in a centrifuge in a 1-g environment. The same method of display is used as in Fig. 3. The motion proceeds further in the  $x$  direction (vertical on the page in TOP VIEW) and further in the  $z$  direction (vertical in RIGHT SIDE VIEW) than does the clockwise simulation in Fig. 3.

tion (forward, here). Interestingly, the computed three-dimensional perception is not the mirror image of that for clockwise head yaw (Fig. 3). In addition, the perceived distance traveled (Fig. 5(b)) is greater during counterclockwise yaw.

Overall, perceptual disturbance is predicted to be greater during counterclockwise yaw than during clockwise yaw because the Stretch Factor is greater during counterclockwise yaw (Fig. 5(b)). In addition, the three-dimensional displays show that pitch perception, in particular, may be greater during counterclockwise yaw because of the greater linear excursion enhancing the pitch perception in the counterclockwise display.

These differences are not predicted by analysis of angular components alone; the Twist Factor is identical for the two movements (Fig. 5(a)).

### 3.2. In zero-g at radius 1 m

Simulations resulted in three-dimensional displays (Figs 6 and 7) and graphs of Twist and Stretch (zero-g

curves in Fig. 5) for self-motion perception in zero-g during the same  $90^\circ$  clockwise and counterclockwise head movements as used for 1-g above.

The computed three-dimensional perceived motion during clockwise (left-to-nose-up) head yaw (Fig. 6) begins with the initial perceived orientation of upright, and proceeds with clockwise yaw into a backward pitch-like motion with turn/rotation. The backward pitch rotation is not accompanied nearly as much by linear motion as in the corresponding 1-g simulation (Fig. 3).

The corresponding simulation during counterclockwise (right-to-nose-up) head yaw (Fig. 7) results in a mirror-image, in a three-dimensional sense, of the simulation during clockwise yaw (Fig. 6). The initial perceived orientation is upright, and the motion proceeds with counterclockwise yaw into a forward pitch-like motion with turn/rotation. Once again, the pitch rotation is not accompanied nearly as much by linear motion as in the corresponding 1-g simulation (Fig. 4).

Although the Twist Factor is identical in all conditions here (Fig. 5(a)), the Stretch Factor differs be-

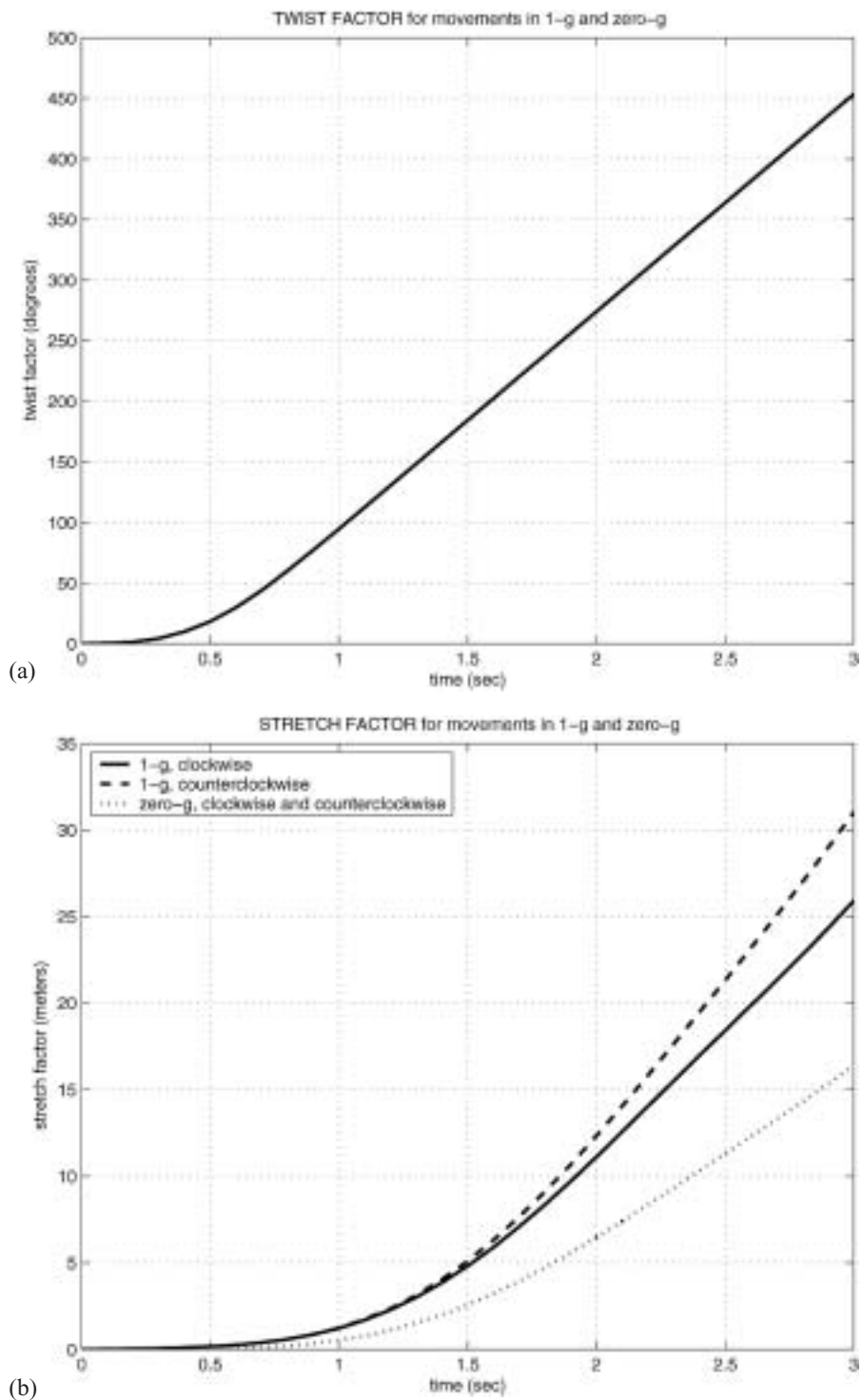


Fig. 5. Twist and Stretch Factors for simulated perceived head motion for 3 s during 1 s of head clockwise and counterclockwise yaw, plus the subsequent 2 s, in a centrifuge in 1-g and zero-g environments. (a) Twist Factor, which is the same for all four movements, both clockwise and counterclockwise in both 1-g and zero-g. The first 1.5 s on this graph correspond to the Twist Factor that arises in each of Figs 3, 4, 6, and 7. (b) Stretch Factor. The first 1.5 s on this graph correspond to the Stretch Factors that arise in Fig. 3 (1-g, clockwise), Fig. 4 (1-g, counterclockwise), and Figs 6 and 7 (zero-g).

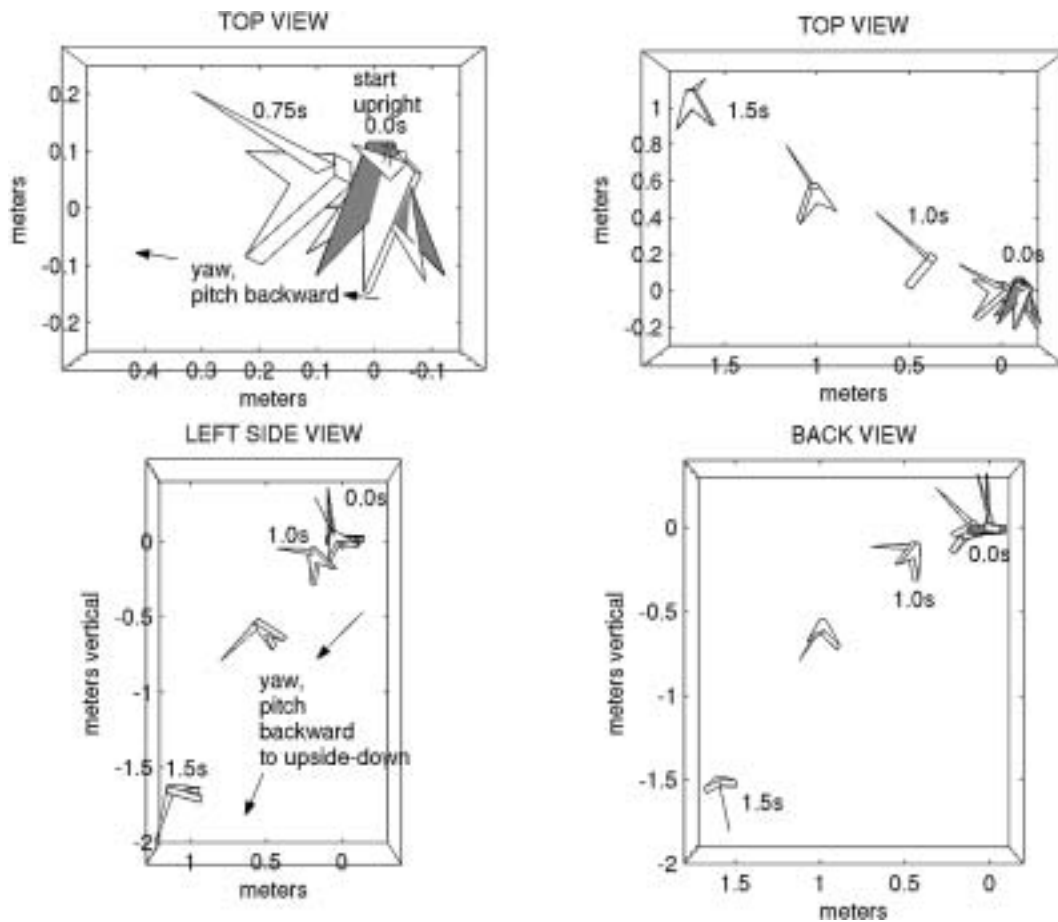


Fig. 6. Clockwise in zero-g: Three-dimensional view of simulated perceived head motion for 1.5 seconds, during 1 s of clockwise (left-to-nose-up) head yaw, plus the subsequent 0.5 s, in a centrifuge in a zero-g environment (details in the text). The same method of display is used as in Fig. 3. The motion is described further in the text.

tween zero-g and 1-g (Fig. 5(b)). The Stretch Factor is smaller in zero-g than in 1-g, predicting that perceptual disturbance may be less for this motion in zero-g than in 1-g. Also, the Stretch Factor in zero-g is the same for clockwise and counterclockwise head yaw, unlike in 1-g where the Stretch Factor is greater for counterclockwise than for clockwise head yaw, in the clockwise-rotating centrifuge.

### 3.3. Standard coriolis versus coriolis in a centrifuge

Three-dimensional simulations for on-axis rotation were distilled down to Twist and Stretch Factors after 3 s for self-motion perception associated with head yaw. This is the type of motion used to produce the “standard” vestibular coriolis effect. In order to make a direct comparison with the centrifuge coriolis effects above, the same orientation and movement of the head

were used as in the 1 m-radius simulations, with 90° head movement in 1 s during 126.9°/s rotation.

The Twist Factors were identical, equaling 453°, in all conditions: 1-g standard coriolis, zero-g standard coriolis, 1-g centrifuge coriolis, and zero-g centrifuge coriolis.

The Stretch Factors differed between conditions:

- Standard coriolis, 1-g: 27.1 m,
- Standard coriolis, zero-g: 0.0 m,
- Centrifuge coriolis, clockwise, 1-g: 25.9 m,
- Centrifuge coriolis, counterclockwise, 1-g: 31.0 m,
- Centrifuge coriolis, zero-g: 16.4 m.

As has been shown previously [18], the standard coriolis condition is thus predicted to produce a much weaker perceptual disturbance in zero-g than in 1-g. In addition, the centrifuge coriolis condition may be predicted to produce a weaker perceptual disturbance in

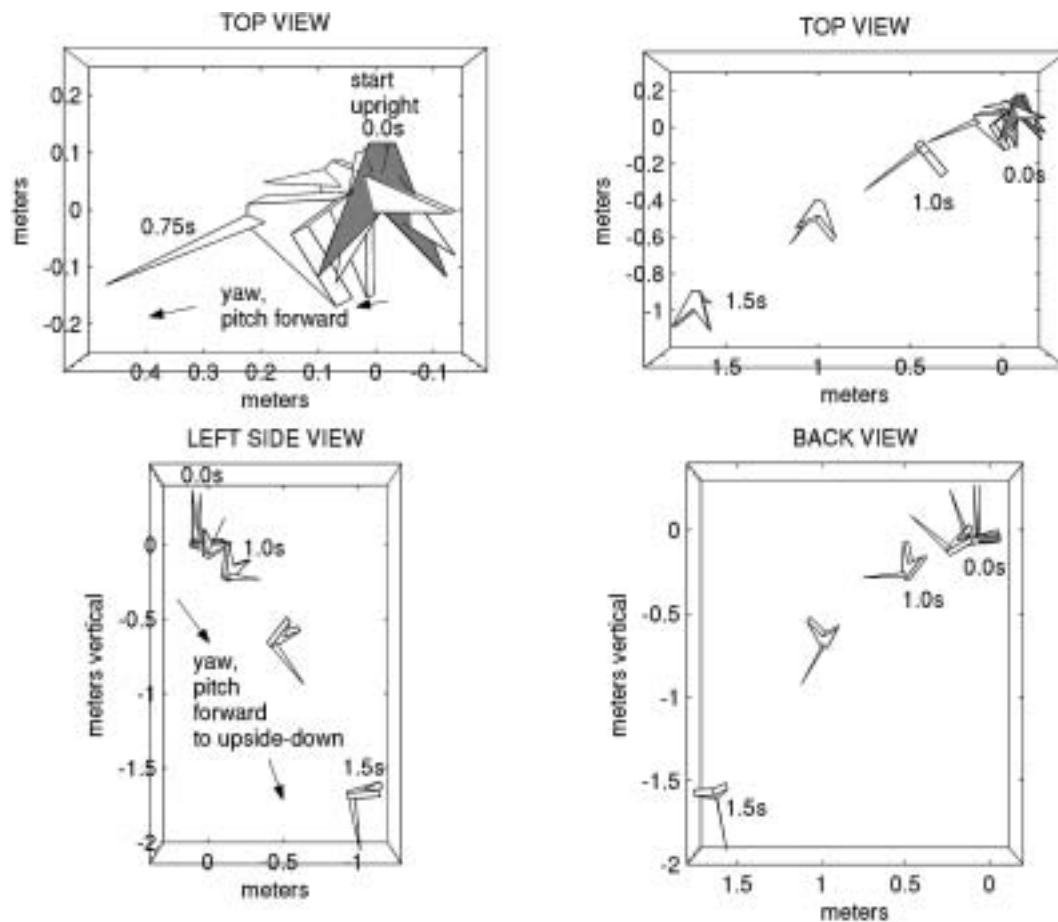


Fig. 7. Counterclockwise in zero-g: Three-dimensional view of simulated perceived head motion for 1.5 seconds, during 1 s of counterclockwise (right-to-nose-up) head yaw, plus the subsequent 0.5 s, in a centrifuge in a zero-g environment. The same method of display is used as in Fig. 3. The motion proceeds in the same manner as in the clockwise simulation in Fig. 6, although directions of perceived motion are different.

zero-g than in 1-g. However, the 1-g-zero-g difference is much less for the centrifuge coriolis condition than for the standard coriolis condition.

In summary, perceptual disturbances from head movements in zero-g are predicted to be greater during centrifugation than during on-axis rotation. The known reduction of the vestibular coriolis effect in zero-g is predicted to apply less during centrifugation.

#### 4. Discussion

Three-dimensional modeling gives three main results regarding self-motion perception during head yaw turns while supine, head toward center, in a clockwise-rotating centrifuge: (1) in a 1-g environment, counterclockwise head yaw is predicted by the laws of physics to give stronger perceptual effects than does clockwise

head yaw, (2) the laws of physics do not show a corresponding clockwise-counterclockwise difference in zero-g, and (3) the model predicts that in zero-g the vestibular coriolis effect will be greater during centrifugation than during on-axis rotation.

The first result turns out to be confirmed by experimental work [14]. Counterclockwise yaw has been shown to give stronger perceptual effects than does clockwise yaw, at least in terms of the magnitude of illusory pitch. In the experiment, the centrifuge rotated clockwise at  $138^\circ/\text{s}$  ( $= 23 \text{ rpm}$ ) with the top of the subject's head at the axis of rotation. Clockwise yaw turns were performed both left-to-nose-up and nose-up-to-right, while counterclockwise yaw turns were performed both right-to-nose-up and nose-up-to-left. Although the present modeling project only investigated turns to nose-up, analysis of the model shows that for a clockwise-rotating centrifuge, any clockwise  $90^\circ$  yaw

turn, regardless of the starting position of the head, gives the same Stretch Factor; similarly, any counterclockwise 90° yaw turn gives the same Stretch Factor. Therefore, for a clockwise-rotating centrifuge, the model predicts stronger perceptual effects for counterclockwise yaw turn than for clockwise yaw turn whenever comparing yaw turns with analogous head-body orientations, so that neck afferent activity, for example, is analogous.

The model thus gives a possible explanation for the experimental result. In addition, the reason for the perceptual asymmetry can be garnered from the three-dimensional display. For clockwise yaw, the illusory pitch orientation begins already tilted back, and the backward pitch proceeds from there (Fig. 3). For counterclockwise yaw, the illusory pitch begins tilted back, which is not the direction of the ensuing illusory pitch motion, and then proceeds pitch forward through an approximately upright orientation in order to continue forward (Fig. 4). These directions of illusory pitch motion depend upon the fact that the centrifuge rotates clockwise. Although computer simulations are required in order to ascertain the exact consequences for Stretch of this asymmetry, the three-dimensional display shows the asymmetry so that it can be translated back into a greater understanding of the original experimental setup: “upright” in the model translates into “direction of the initial GIA” in the experiment. The subject always begins with the GIA pointing – from the point of view of the subject’s body – diagonally upward and forward. The illusion associated with clockwise head yaw pitches the body axis away from the GIA, while the illusion associated with counterclockwise head yaw pitches the body axis toward the GIA. This asymmetry, brought to light by three-dimensional modeling, is thus understandable simply in terms of the relative directions of the GIA and the illusory pitch.

Further investigation along these lines is possible. One point of consideration is subjects’ perceived orientation preceding the head turn. While the current modeling project used simulated subjects who perceived the GIA as vertical, some subjects in experimental research have reported orientations even as extreme as upright or almost supine [13]. A clockwise-counterclockwise asymmetry would still be expected to appear, however, because the motion itself has an asymmetry in the relative directions of the GIA and the illusory pitch. The consequences of this asymmetry for different initial perceived orientations remains to be tested. Another line of investigation could test different axes of head movement. In one study [38], differences in mo-

tion sickness were marginally significant during pitch up versus pitch down while seated facing out in a centrifuge; in addition, differences during standard coriolis versus centrifuge coriolis were not significant, just as the present modeling study predicts for yaw while supine (Stretch Factors: Standard Coriolis 27.1 m, Centrifuge Coriolis 25.9 m for clockwise and 31.0 m for counterclockwise).

The second main modeling result, that a clockwise-counterclockwise asymmetry does not appear in zero-g by the laws of physics, could someday be followed up experimentally. The three-dimensional computations here could be used as “baselines” [16,17] from which physiological asymmetries (or lack thereof) could be identified. On the one hand, if human subjects in zero-g do not report the clockwise-counterclockwise differences that appear in 1-g, then the laws of physics explain this dissimilarity between 1-g and zero-g. On the other hand, if subjects in zero-g do report clockwise-counterclockwise differences, then a human perceptual asymmetry is responsible. An asymmetry might arise, for example, by means of forward-backward differences in magnitude of the illusory perception of pitch.

The third result states that in zero-g, stronger perceptual effects are predicted in a centrifuge than during on-axis rotation. This result arises from analysis of the Stretch Factor, which had been used successfully to give an explanation for the weaker vestibular coriolis effect in zero-g as compared to 1-g [18]. The present prediction is robust; preliminary testing shows that variations in the parameters of the motion and of the model lead to the same result: effects in zero-g are stronger in the centrifuge than on-axis.

The model also compares centrifugation in zero-g with centrifugation in 1-g. The Stretch Factor for the centrifuge coriolis condition is less in zero-g than in 1-g (though not nearly as small as for the standard coriolis condition in zero-g). However, this result is less robust than is the “third” result above. In comparing centrifugation between zero-g and 1-g, an assumption about adaptation to zero-g was necessary when the level of “gravity” was set to 0.5 g (equal to the magnitude of the GIA) in the model. By this means, the model effectively simulated a subject who interpreted the GIA as being a gravity vector. A similar situation occurs in centrifuges on the earth: subjects typically interpret the GIA as being the gravity vector even though it has unusual magnitude (greater than 1 g). Nevertheless, further experimental research on orientation in centrifuges, along lines that have already been started in zero-g [3,7], would be necessary to fine-tune the mod-

el's perceptual interpretation of the 0.5 g-magnitude GIA. In one set of experiments [7], subjects in a centrifuge with 0.5 g or 1 g centripetal acceleration often reported a perception of tilt that was not aligned with the GIA, especially early in flight. The only result in the present paper that depends on this fine-tuning is the 1-g-zero-g centrifuge comparison: depending on the exact interpretation of the 0.5 g vector, the perceptual disturbance in a centrifuge in zero-g may be of similar magnitude to that in 1-g or may be less, but is not predicted by the model to be as reduced as is the standard vestibular coriolis effect.

For all of the results of the present research, an obvious question is whether the results still hold if the model were to incorporate known time constants associated with human perception. The answer is 'yes'. One reason is that the time frame used here is short, 3 s at the most, so time constants do not have as much of an effect as they would for longer time periods. Another reason is that the results here are about relative magnitudes of perceptual disturbances, and time constants affect all simulations in a similar way. For further confirmation of these facts, the present three-dimensional model has been extended to make available parameters for three time constants: for decay of angular motion perception, for decay of linear motion perception, and for tilt, i.e. reorientation so that the subjective vertical approaches the resultant linear vector. With this extended model, relative magnitudes of the Twist and Stretch Factors between conditions were tested for vestibular coriolis effects during simulations with time constants included, 20 s for angular, 0.5 s for linear, and 5 s for tilt. The relative magnitudes, between conditions, of the Twist and Stretch Factors did not change [19], and the same results have held when further tested with other values for the time constants in ranges 10–20 s for angular, 0.5–5 s for linear, and 2–5 s for tilt. Centrifuge runs have been tested as well, and the type of three-dimensional perception remained the same.

The present model has similarities and differences with other three-dimensional models [1,2,5,6,8,9,20,24–29,33–37,40]. The focus on pure physics is one way in which the present model (also in [16,17]) differs from the others, which combine physics and physiological factors. The focus here on physics is purposeful, to separate out perceptual phenomena that can be explained by the laws of physics from those that must involve unique properties of a physiological system. Though the present model could have been run with time constants, making it more similar to other models, the pure laws-of-physics implementation clarified a source of

clockwise-counterclockwise differences in magnitude of perceptual effects. It was necessary to use this model with straight three-dimensional laws of physics in order to discover that the asymmetry was not purely physiological.

At the same time, this model shares a structural similarity with many others. Because the present model follows the laws of physics and therefore keeps track of values of the variables, including linear acceleration and "gravitational acceleration" which sum to the GIA, this model can be said to incorporate an internal model (e.g. [28]). Indeed, the present model uses its current state in its computation of next states, as always happens in systems of differential equations such as those of the laws of physics.

The present model differs from others, however, in its method of display, a three-dimensional display. This display is possible because the model keeps track of all orientation information relative to the surroundings, not just gravity ( $\vec{g}$ ). The model keeps track of three-dimensional orientation in terms of  $\vec{i}$ ,  $\vec{j}$ , and  $\vec{k}$  vectors, and includes a computation of linear position. These variables and computations were included because the model was developed to investigate fully three-dimensional perception, and the results are displayed as such.

Finally, Twist and Stretch Factors have been extracted in order to make analysis of the three-dimensional graphs more accessible. This is not to say that a more sophisticated mathematical analysis would not be possible. A mathematical model of the connection between movement and motion sickness, for example, has been developed [32].

In conclusion, a three-dimensional model can help make predictions about perceptual disturbances in zero-g. The model can aid in research on zero-g, while at the same time, experimental research can aid in fine-tuning the design of the model. Experimental and modeling research are complementary, especially as research on self-motion perception delves into more complex motions and more difficult-to-study motion environments.

## Acknowledgements

Thanks to Sarah Pierce, John Kuehne, and Faith Anderson for technical assistance. Two anonymous reviewers gave valuable suggestions for better communicating various points. This research was supported by the Clare Boothe Luce Fund administered by the Henry Luce Foundation and by the Colby College Natural Sciences Grant Program.

## References

- [1] D.E. Angelaki, D.M. Merfeld and B.J.M. Hess, Low-frequency otolith and semicircular canal interactions after canal inactivation, *Experimental Brain Research* **132** (2000), 539–549.
- [2] D.E. Angelaki, M. Wei and D.M. Merfeld, Vestibular discrimination of gravity and translational acceleration, *Annals of the New York Academy of Sciences* **942** (2001), 114–127.
- [3] A.J. Benson, F.E. Guedry, D.E. Parker and M.F. Reschke, Microgravity vestibular investigations: perception of self-orientation and self-motion, *Journal of Vestibular Research* **7** (1997), 453–457.
- [4] W. Bles, Coriolis effects and motion sickness modelling, *Brain Research Bulletin* **47** (1998), 543–549.
- [5] J. Borah, L.R. Young and R.E. Curry, Optimal estimator model for human spatial orientation, *Annals of the New York Academy of Sciences* **545** (1988), 51–73.
- [6] J.E. Bos and W. Bles, Theoretical considerations on canal-otolith interaction and an observer model, *Biological Cybernetics* **86** (2002), 191–207.
- [7] G. Clément, S.T. Moore, T. Raphan and B. Cohen, Perception of tilt (somatogravic illusion) in response to sustained linear acceleration during space flight, *Experimental Brain Research* **138** (2001), 410–418.
- [8] J. Droulez and C. Darlot, The geometric and dynamic implications of the coherence constraints in three-dimensional sensorimotor interactions, in: *Attention and Performance*, M. Jeanerod, ed., Lawrence Erlbaum, Hillsdale, NJ, 1989, pp. 495–526.
- [9] S. Glasauer and D.M. Merfeld, Modelling three-dimensional vestibular responses during complex motion stimulation, in: *Three-Dimensional Kinematics of Eye, Head and Limb Movements*, M. Fetter, T. Haslwanter, H. Misslich and D. Tweed, eds, Harwood, Reading, 1997, pp. 387–398.
- [10] A. Graybiel, E.F. Miller and J.L. Homick, Experiment M131. Human vestibular function, in: *Biomedical Results from Skylab*, (Section II), R.S. Johnston and L.F. Dietlein, eds, NASA SP-377, US Government Printing Office, 1977, pp. 74–103.
- [11] F.E. Guedry, Jr., Psychophysics of vestibular sensation, in: *Handbook of Sensory Physiology*, (Vol. VI), H.H. Kornhuber, ed., Springer, Berlin, 1974, pp. 3–154.
- [12] F.E. Guedry, Jr. and A.J. Benson, Coriolis cross-coupling effects: disorienting and nauseogenic or not? *Aviation, Space, and Environmental Medicine* **49** (1978), 29–35.
- [13] Heiko Hecht, personal communication.
- [14] H. Hecht, J. Kavelaars, C.C. Cheung and L.R. Young, Orientation illusions and heart-rate changes during short-radius centrifugation, *Journal of Vestibular Research* **11** (2001), 115–127.
- [15] J.E. Holly, Subject-coincident coordinate systems and sustained motions, *International Journal of Theoretical Physics* **35** (1996), 445–473.
- [16] J.E. Holly, Three-dimensional baselines for perceived self-motion during acceleration and deceleration in a centrifuge, *Journal of Vestibular Research* **7** (1997), 45–61.
- [17] J.E. Holly, Baselines for three-dimensional perception of combined linear and angular self-motion with changing rotational axis, *Journal of Vestibular Research* **10** (2000), 163–178.
- [18] J.E. Holly, Three-dimensional differences between vestibular coriolis effects during acceleration, deceleration, and microgravity, *Society for Neuroscience Abstracts* **26** (2000), 1495.
- [19] J.E. Holly, Linear-angular interactions modeled in three dimensions to identify disorienting vestibular-proprioceptive mismatch, in: *Abstracts of Multisensory Interactions Subserving Orienting Behavior (Satellite to Neural Control of Movement, 12th Annual Meeting)*, Naples, Florida, USA, April 14–16, 2002.
- [20] K. Kushiro, M. Dai, M. Kunin, S.B. Yakushin, B. Cohen and T. Raphan, Compensatory and orienting eye movements induced by off-vertical axis rotation (OVAR) in monkeys, *Journal of Neurophysiology* **88** (2002), 2445–2462.
- [21] J.R. Lackner and P. DiZio, Multisensory, cognitive, and motor influences on human spatial orientation in weightlessness, *Journal of Vestibular Research* **3** (1993), 361–372.
- [22] J.R. Lackner and A. Graybiel, The effective intensity of coriolis, cross-coupling stimulation is gravito-inertial force dependent: implications for space motion sickness, *Aviation, Space, and Environmental Medicine* **57** (1986), 229–235.
- [23] G. Melvill Jones, Origin significance and amelioration of coriolis illusions from the semicircular canals: a non-mathematical appraisal, *Aerospace Medicine* **41** (1970), 483–490.
- [24] D.M. Merfeld, Modeling human vestibular responses during eccentric rotation and off vertical axis rotation, *Acta Otolaryngologica, Supplement* **520** (1995), 354–359.
- [25] D.M. Merfeld, Modeling the vestibulo-ocular reflex of the squirrel monkey during eccentric rotation and roll tilt, *Experimental Brain Research* **106** (1995), 123–134.
- [26] D.M. Merfeld, L.R. Young, C.M. Oman and M.J. Shelhamer, A multidimensional model of the effect of gravity on the spatial orientation of the monkey, *Journal of Vestibular Research* **3** (1993), 141–161.
- [27] D.M. Merfeld and L.H. Zupan, Neural processing of gravito-inertial cues in humans. III. Modeling tilt and translation responses, *Journal of Neurophysiology* **87** (2002), 819–833.
- [28] D.M. Merfeld, L. Zupan and R.J. Peterka, Humans use internal models to estimate gravity and linear acceleration, *Nature* **398** (1999), 615–618.
- [29] T. Mergner and S. Glasauer, A simple model of vestibular canal-otolith signal fusion, *Annals of the New York Academy of Sciences* **871** (1999), 430–434.
- [30] H. Mittelstaedt, Somatic graviception, *Biological Psychology* **42** (1996), 53–74.
- [31] M.-L. Mittelstaedt and H. Mittelstaedt, The influence of otoliths and somatic graviceptors on angular velocity estimation, *Journal of Vestibular Research* **6** (1996), 355–366.
- [32] C.M. Oman, A heuristic mathematical model for the dynamics of sensory conflict and motion sickness, *Acta Otolaryngologica, Supplement* **392** (1982).
- [33] C.C. Ormsby and L.R. Young, Integration of semicircular canal and otolith information for multisensory orientation stimuli, *Mathematical Biosciences* **34** (1977), 1–21.
- [34] T. Raphan and B. Cohen, The vestibulo-ocular reflex in three dimensions, *Experimental Brain Research* **145** (2002), 1–27.
- [35] T. Raphan and D. Sturm, Modeling the spatiotemporal organization of velocity storage in the vestibuloocular reflex by optokinetic studies, *Journal of Neurophysiology* **66** (1991), 1410–1421.
- [36] G. Reymond, J. Droulez and A. Kemeny, Visuovestibular perception of self-motion modeled as a dynamic optimization process, *Biological Cybernetics* **87** (2002), 301–314.
- [37] S. Wearne, T. Raphan and B. Cohen, Effects of tilt of the gravito-inertial acceleration vector on the angular vestibuloocular reflex during centrifugation, *Journal of Neurophysiology* **81** (1999), 2175–2190.
- [38] P.D. Woodman and M.J. Griffin, Effect of direction of head movement on motion sickness caused by coriolis stimulation,

- Aviation, Space, and Environmental Medicine* **68** (1997), 93–98.
- [39] L.R. Young, Perception of the body in space: mechanisms, in: *Handbook of Physiology*, Volume III (Sensory Processes, Part 2), I. Darian-Smith, ed., American Physiological Society, Bethesda, Maryland, 1984, pp. 1023–1066.
- [40] L.H. Zupan, D.M. Merfeld and C. Darlot, Using sensory weighting to model the influence of canal, otolith and visual cues on spatial orientation and eye movements, *Biological Cybernetics* **86** (2002), 209–230.